

Melting Behavior of Polymorphics: Molecular Weight Dependence and Steplike Mechanisms in Nylon-6

F. J. Medellín-Rodríguez,^{*,†} L. Larios-López,[†] A. Zapata-Espinoza,[†]
O. Dávalos-Montoya,[†] P. J. Phillips^{‡,§}, and J. S. Lin[§]

CIEP-FCQ-UASLP, Av. Dr. Manuel Nava 6, Zona Universitaria 78210,
San Luis Potosí, S.L.P., México; MSE Department, University of Tennessee,
Knoxville, Tennessee 37996-2200; and Oak-Ridge National Laboratory, Solid State Division,
Oak Ridge, Tennessee 37831

Received September 4, 2003

ABSTRACT: The effect of molecular weight on the isothermal crystallization and complex melting behavior of polymorphic nylon-6 has been studied within the context of the steplike crystallization and melting mechanism. Quiescent isothermal crystallization, at relatively low crystallization temperatures, of low molecular weight nylon-6 samples, although poorly defined, predominantly developed the α crystalline form. Linear heating of these samples gave place to a single melting endotherm. An increase in crystallization temperature developed a better-defined α form with the single melting behavior continuing up to temperatures where a small endotherm appeared immediately after the crystallization temperature. A sequential increase of crystallization temperature (paralleled by increased definition of the α crystalline form) rendered triple melting behavior. This latter phenomenon was followed by the return of double melting at the expense of the third melting endotherm after isothermal crystallization at higher temperatures. High molecular weight samples predominantly developed the γ form at low isothermal crystallization temperatures, the melting behavior giving rise to the formation of a new melting endotherm with melting point slightly lower than the high endotherm previously observed with the low molecular weight sample. In addition, there was also the formation of a lower amount of a third melting endotherm. On the basis of these results, an explanation is given for each melting endotherm. It was also determined that, on heating, nylon-6 can recrystallize from the less stable γ form to the more stable α form within a process parallel to melting. From a comparison of the crystallization results for different molecular weights, under the stable α crystal habit, it was determined that the basic concepts of the steplike crystallization and melting mechanism can also be applied to the complex melting behavior of the polymorphic nylon-6.

Introduction

Nylon-6 is an important engineering polymer, which is able to crystallize in at least two crystal habits depending on crystallization conditions. The more thermodynamically stable α form consists of molecules in an extended chain conformation with hydrogen bonds between antiparallel chains. This can be achieved by adjacent reentry of the folded chains into the crystal.^{1,2} The γ form consists of chains in an extended conformation but having hydrogen bonding between parallel chains.^{2,3} This last form is typically obtained in transformations involving uniaxial deformation. Both the α and γ crystalline forms can be generated as a function of supercooling and annealing. The melting behavior of isothermally crystallized nylon-6 has been reported in the past,^{4–9} and multiple melting is commonly observed in differential scanning calorimetry (DSC) traces. However, such behavior is atypical, and as a consequence, several hypotheses have been proposed to explain the observed results. These have included continuous recrystallization events during the DSC scan^{4–6} and different crystalline structures associated with the particular melting endotherms when the crystallization temperature is changed.^{7,8} However, it has also been proposed that the melting behavior of nylons could be exclusive to this family of polymers.⁹

In the recent past, the crystallization and melting behavior of high-temperature polymers has been explained in terms of the steplike crystallization and melting mechanism,¹⁰ which is basically a morphological explanation. On the basis of this model, evidence was given to explain the triple melting behavior of poly(ethylene terephthalate) (PET) homopolymers¹¹ and random poly(ethylene terephthalate)-*co*-1,4-cyclohexylene dimethylene terephthalate (PET/CT) copolymers.¹² The steplike melting mechanism was also considered for use with these and other semicrystalline polymers. Nylon-6 is, however, a more complicated system because of its polymorphism. Nevertheless, the purpose of the present study is to analyze the general characteristics of crystallization and melting of nylon-6 and to show that the complex melting behavior of this polymer can also be explained within the context of the steplike crystallization and melting mechanism.

Experimental Section

Materials and Methods. Nylon-6 samples with a number-average molecular weight of 16 000 and 35 000 g/mol were obtained from Polysciences, Inc. Their relative viscosities were 2.4 and 4.1 for intrinsic viscosities of 0.999 and 1.866 dL/g, respectively, which corresponded to viscous average molecular weights of 27 922 and 59 804 g/mol, respectively.

Differential Scanning Calorimetry. All nylon-6 samples were first dried under vacuum for 3.5 h at 40 °C before any experimentation. Differential scanning calorimetry (DSC) traces were taken after isothermally crystallizing samples at different temperatures. Samples weighting 6–8 mg were placed in aluminum sample holders and then in a Perkin-Elmer DSC-7 calorimeter where they were heated at the

* Corresponding author. E-mail: francmr@uaslp.mx.

† CIÉP-FCQ-UASLP.

‡ University of Tennessee.

§ Oak-Ridge National Laboratory.

‡ Present address: Department of Chemical and Materials Engineering, University of Cincinnati, 400 Rhodes Hall, P.O. Box 210012, Cincinnati, OH 45221-0012.

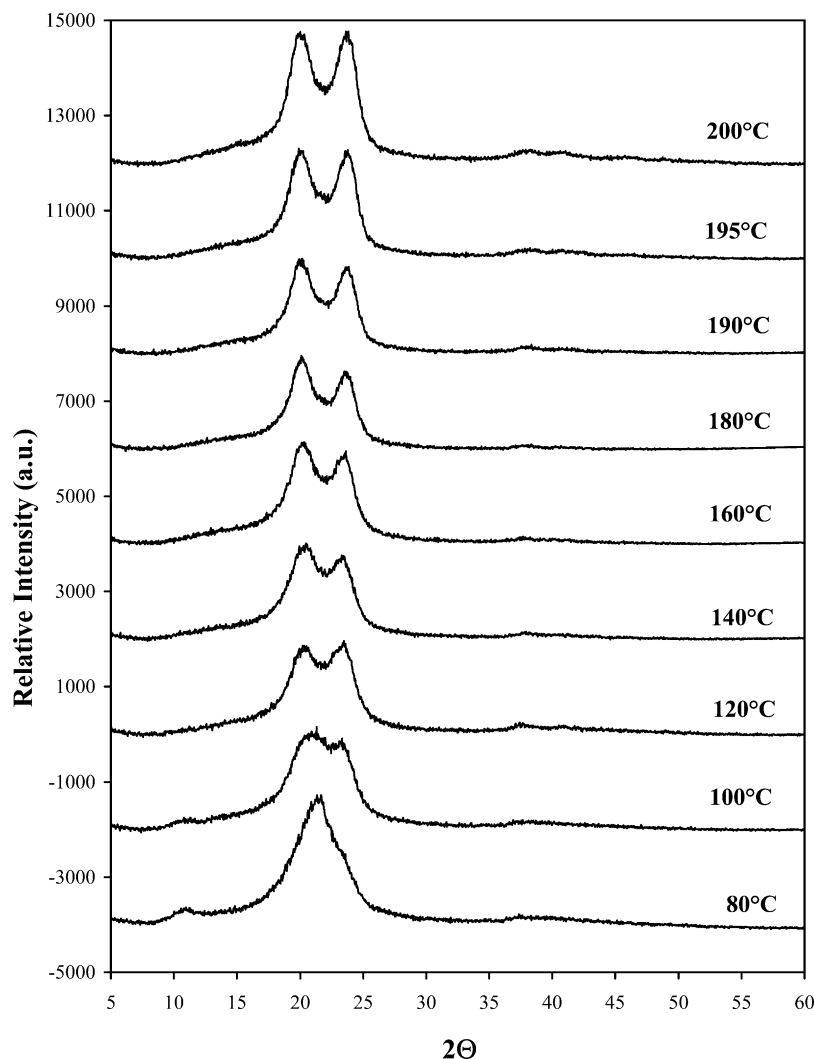


Figure 1. WAXD patterns of low molecular weight nylon-6 after isothermal crystallization (1 h) at the indicated temperatures.

reported equilibrium melting temperature of 260 °C¹³ for 3 min. Samples were quenched directly from the molten state at the nominal rate of 500 °C/min to the crystallization temperature, where they remained for 60 min. They were then heated directly at the rate of 10°/min from the crystallization temperature up to the equilibrium melting temperature in order to register the melting curve.

Polarized Optical Microscopy. Polarized optical microscopy (POM) was used to register morphological changes (in terms of micrographs and transmitted light) during heating. Samples with an average thickness of 60 μm were placed between two glass slides and were heated at 260 °C in a FP82HT Mettler hot stage where they remained for 3 min. The molten sample was quickly transferred to the crystallization hot stage, already set at the desired crystallization temperature, and placed in a polarizing Olympus optical microscope, where it remained for 1 h. The sample was linearly heated from the isothermal crystallization temperature, the transmitted light intensity being recorded with a photodetector (Mettler ZUFP82HT).

Wide-Angle X-ray Diffraction. Specimens used for X-ray diffraction/scattering experiments were prepared using the fast-transfer technique. In this case, plates with dimensions 1 × 1 × 0.05 cm were melted and crystallized using two Mettler FP82HT hot stages. One of them was at the equilibrium melting temperature and the other at the crystallization temperature and both under a controlled flux of nitrogen of 500 cm³/min. WAXD patterns were obtained in a Rigaku DMAX B-2200 diffractometer. Samples were first melted, then crystallized, and then quenched between cold metal surfaces at 3 °C. The corresponding WAXD patterns were collected in

transmission mode at room temperature using a tube current of 30 mA and an acceleration voltage of 40 kV. The range of the diffracting 2θ angle was 5°–60°, and the scanning rate was 3°/min.

Small-Angle X-ray Scattering. The experiments were performed on the ORNL 10 m SAXS instrument^{14,15} using two sample-to-detector distances of 1.119 and 5.119 m, Cu Kα radiation ($\lambda = 1.54$ Å), and a 20 × 20 cm² two-dimensional position-sensitive area detector with each virtual cell (element) size about 3 mm apart. Corrections were made for instrumental backgrounds, dark current due to cosmic radiation and electronic noises in the detector circuitry, detector nonuniformity, and efficiency (via an ⁵⁵Fe radioactive isotope standard which emits X-rays isotropically by electron capture) on a cell-by-cell basis. The data were radially (azimuthally) averaged in the q range $0.1 \leq q \leq 4.9$ Å⁻¹ [$q = (4\pi/\lambda) \sin(\theta/2)$], where λ is the X-ray wavelength and θ is the scattering angle, and converted to an absolute differential scattering cross section by means of precalibrated secondary standards. The absolute scattering intensity was in cm⁻¹ units.

Theoretical Considerations. The scattering data, in terms of the intensity of dispersion $I(q)$ and the scattering vector q in reciprocal space, were corrected in order to extrapolate both ends of the scattering curve to $q = 0$ and $q = \infty$, the purpose being to calculate the corrected total scattering intensity or invariant Q and the one-dimensional interface distribution function $g_1(r)$. The Debye¹⁶ model was used to obtain data for the low q range, and the correction was made through $I(q)|_{q \rightarrow 0} = A/(1 + (\epsilon^2 q^2)^2)$, where A is a constant and ϵ is an inhomogeneity length. The high q range was corrected using Porod's law.¹⁷ This applies to an ideal system with

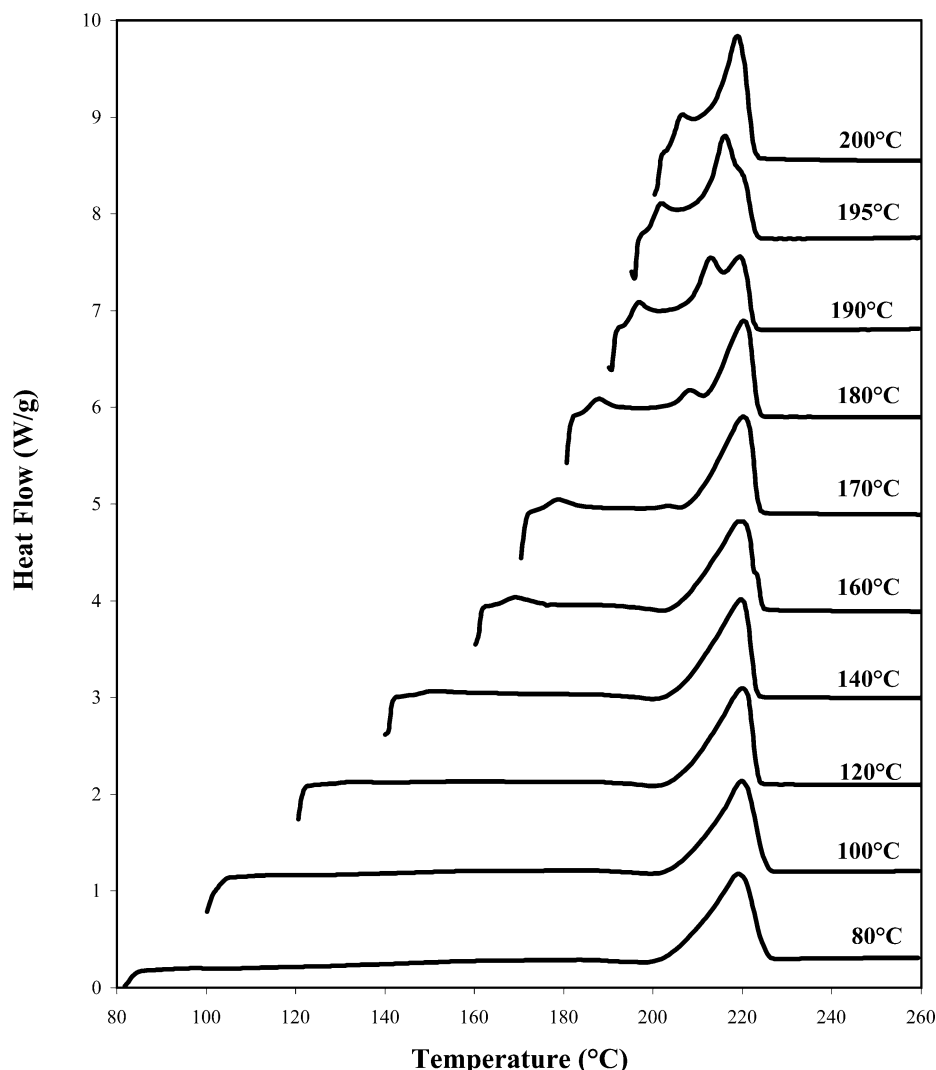


Figure 2. DSC melting traces of low molecular weight nylon-6 after isothermal crystallization (1 h) at the indicated temperatures.

uniform density within each phase and a sharp boundary between phases.¹⁸ In this case, the intensity of dispersion $I(q)$ should inversely change with the fourth power of the scattering vector q or $I(q)|_{q \rightarrow \infty} = K_P/q^4$, where K_P is Porod's constant.

Once the measured data were corrected, the invariant Q was calculated through

$$Q = \int_0^\infty I(q) q^2 dq \quad (1)$$

and the one-dimensional interface distribution function¹⁸ with

$$g_1(r) = \frac{t}{2\pi^2 V} \int_0^\infty G_1(q) \cos(qr) dq \quad (2)$$

where $G_1(q)$ is the interference function given by $G_1(q) = K_P - q^4 I(q)$.

Results

The effect of molecular weight on the diffraction patterns together with a comparison with double melting traces was first reported in 1975 by Gurato et al.¹⁹ In agreement with our results, these authors located the γ/α transitions at 100 °C for low molecular weight samples and at 170 °C for high molecular weight samples.

γ/α transformations can also be caused by stretching, water playing a catalyst role for the transition to occur at higher temperatures.²⁰ Another view for the conver-

sion has been given in terms of an intermediate metastable state whose reversibility depends on a critical value of stress.²¹ In the present study, we are considering quiescent materials; therefore, correlations with the indicated results would only be possible under such conditions. For example, it has been shown before²⁰ that, in the absence of stress, a γ -phase crystal should be transformed into an α -phase crystal at about 220 °C for wet fibers and 300 °C for dry fibers. This is not the case in the results presented in the next paragraphs where transitions are shown to occur at much lower temperatures. Regarding the intermediate metastable state,²¹ even though there is nothing that allows to connect such study with the one here presented, it has to be realized however that, overall, there is a γ/α quiescent transition, as will be shown later, which depends on molecular weight and whose nature seems to be metastable.

Isothermal Crystallization and Melting of Low Molecular Weight. WAXD patterns of low molecular weight (16 000 g/mol) nylon-6 samples, crystallized for 1 h at the indicated temperatures, are shown in Figure 1. One characteristic feature of these patterns is the formation of a poorly defined α crystalline structure at low crystallization temperatures (100 °C). The corresponding DSC traces in Figure 2 indicate a single melting endotherm, resulting from this pseudo- α crystalline structure.

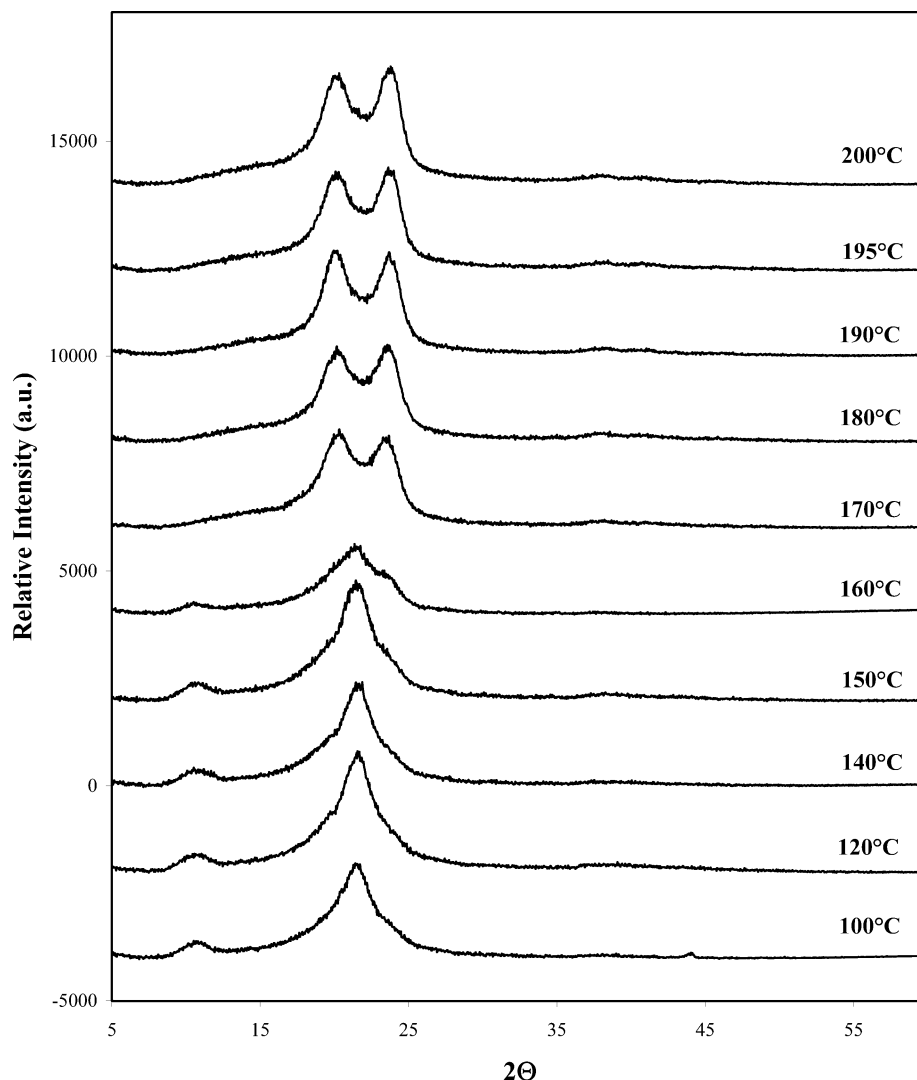


Figure 3. WAXD patterns of high molecular weight nylon-6 after isothermal crystallization (1 h) at the indicated temperatures.

An increase in crystallization temperature, from 100 to 160 °C, gave place to the gradual formation of a better-defined α crystalline structure in the WAXD patterns. The formation of the two characteristic diffracting planes (200) at $2\theta = 20^\circ$ and (002/202) at $2\theta = 24^\circ$ is progressive up to 160 °C, with a tendency of the two diffraction peaks to separate from each other as the crystallization temperature increases. The latter temperature is associated with the beginning of a sequence of triple melting behavior in the DSC traces of Figure 2. In particular, a continuous increase of the second melting endotherm at 203 °C can be clearly seen for crystallization temperatures above 170 °C.

These results indicate that the melting behavior of low molecular weight isothermally crystallized nylon-6 involves from one to three melting endotherms depending on the crystallization temperature. In general, there is a single melting endotherm (III) after crystallization at low temperatures, double melting (I–III) above 140 °C, and triple melting (I–II–III) starting above 160 °C through the formation of an almost imperceptible second melting endotherm. The triple melting sequence reverts around 200 °C to double melting behavior due to the combination of an increase of endotherm II with a decrease of endotherm III. The continuation of the melting process, after isothermal crystallization at still higher temperatures, is expected to generate single

melting, but now due to either the convolution of endotherm I and endotherm II or the disappearance of endotherm I. This latter type of behavior has been observed in PET.¹¹

Isothermal Crystallization and Melting of High Molecular Weight. An increase in the molecular weight (35 000 g/mol) of nylon-6 generated the WAXD patterns shown in Figure 3. The γ form is now obtained at low isothermal crystallization temperatures and over a wide temperature range (100–150 °C). Considering the characteristics of this last crystalline form, where the molecules are in extended chain conformation, the increase in molecular weight seems to make it more difficult for the molecular segments to fold back on themselves rendering a higher amount of extended-like-chain crystals, i.e., those associated with the γ form. There is also a γ/α transition around 160 °C and then a sharp evolution toward the formation of the more stable α form at high crystallization temperatures (170–200 °C). DSC heating traces of the corresponding isothermal crystallization experiments are shown in Figure 4.

Here is clearly observed the influence of molecular weight on the melting behavior. The first low melting endotherm increases gradually with crystallization temperature in a manner similar to the low molecular weight sample; therefore, as a first option it was considered independent. Nevertheless, we determined,

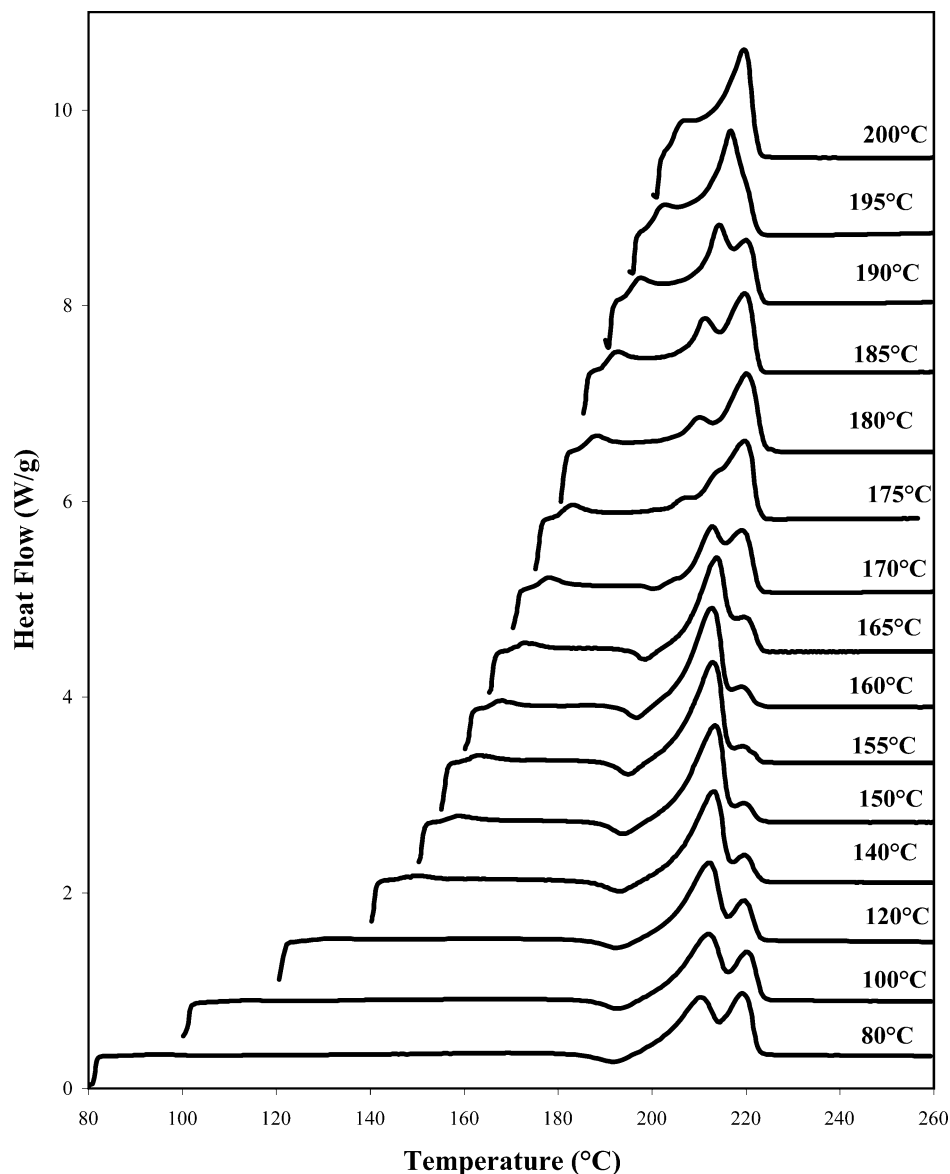


Figure 4. DSC melting traces of high molecular weight nylon-6 after isothermal crystallization (1 h) at the indicated temperatures.

although not shown here, that this first melting endotherm is time dependent, just as in PET,²² and so can be considered morphology related, and most probably associated with the late stages of crystallization. Following endotherm I, there is a recrystallization exotherm at 195 °C, deeper than the one observed with the low molecular weight sample (see specific analyses later). The gradual formation of an additional melting endotherm (II) with a melting point of 212 °C is the next characteristic feature of the melting process. It is also observed that, as the crystallization temperature increases, the second endotherm increases at the expense of the third endotherm within a first melting sequence which ends at about 150 °C. If, as a first option, a correlation is made between the DSC and the WAXD results of the high molecular weight sample, it could be wrongly concluded that double and triple melting can also be generated with the γ form (see later discussion).

Next, at 160 °C and coincident with the γ/α transition in the WAXD patterns (where up to four melting endotherms can be observed), there is an inversion of melting behavior where the second melting endotherm now decreases and the third increases (particularly within the range 155–175 °C). After this transition, the

formation of a better defined α form in the WAXD patterns occurs, and there is triple melting behavior in the DSC traces, similar to that of the first sequence in this high molecular weight sample, or even more, very similar to that observed with the low molecular weight sample.

Discussion

The experimental data show evidence of an unexplained melting sequence in low and high molecular weight samples originating from different crystalline structures. Therefore, the first question to be answered is if the DSC traces were the result of the heating process or if they were directly associated with the original isothermally produced crystals.

In the past, we have proposed several arguments to explain the results of thermal scanning of polymers having a single-crystal habit.^{10–12} Here, however, there is polymorphism involved, which complicates interpretations. Therefore, to understand the melting evolution, we heated the isothermal crystals of the high molecular weight sample, i.e., those that rendered the metastable γ crystalline form, and recorded the WAXD patterns

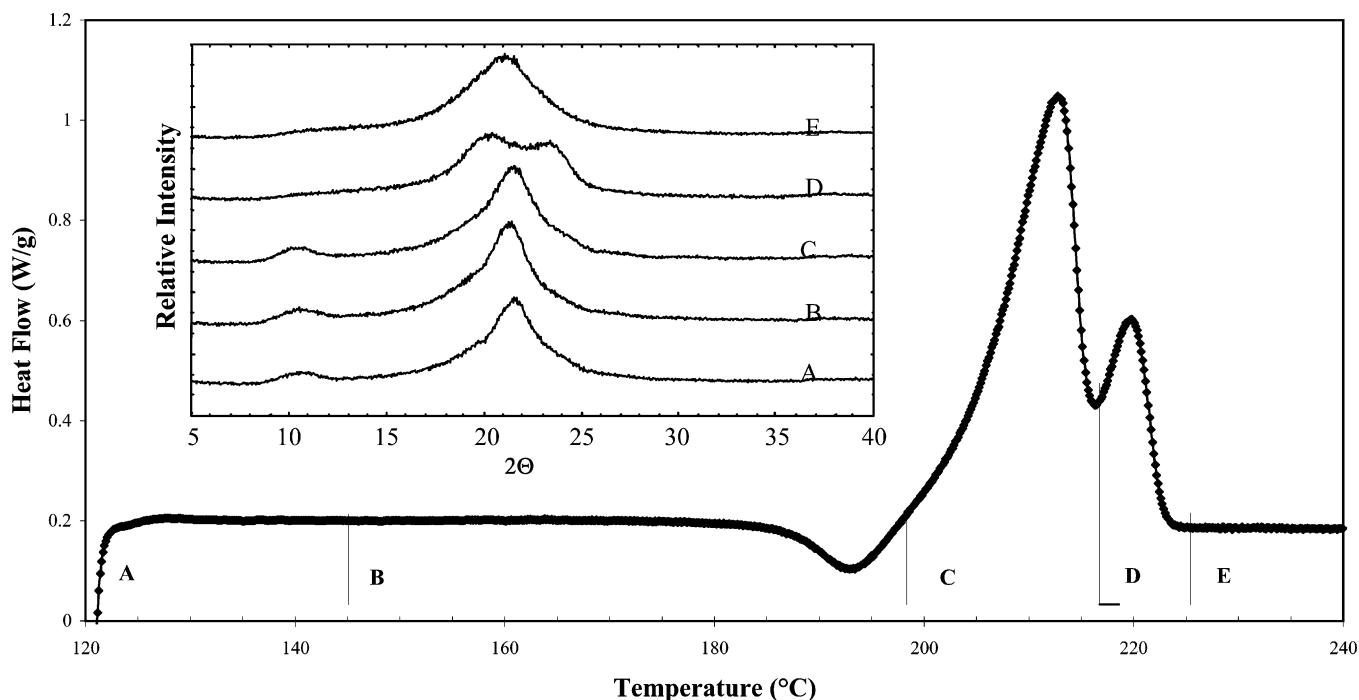


Figure 5. DSC heating trace of high molecular weight nylon-6 after isothermal crystallization (120 °C; 60 min). Inset: WAXD patterns taken at different heating temperatures: (A) 120, (B) 145, (C) 199, (D) 216, and (E) 125 °C.

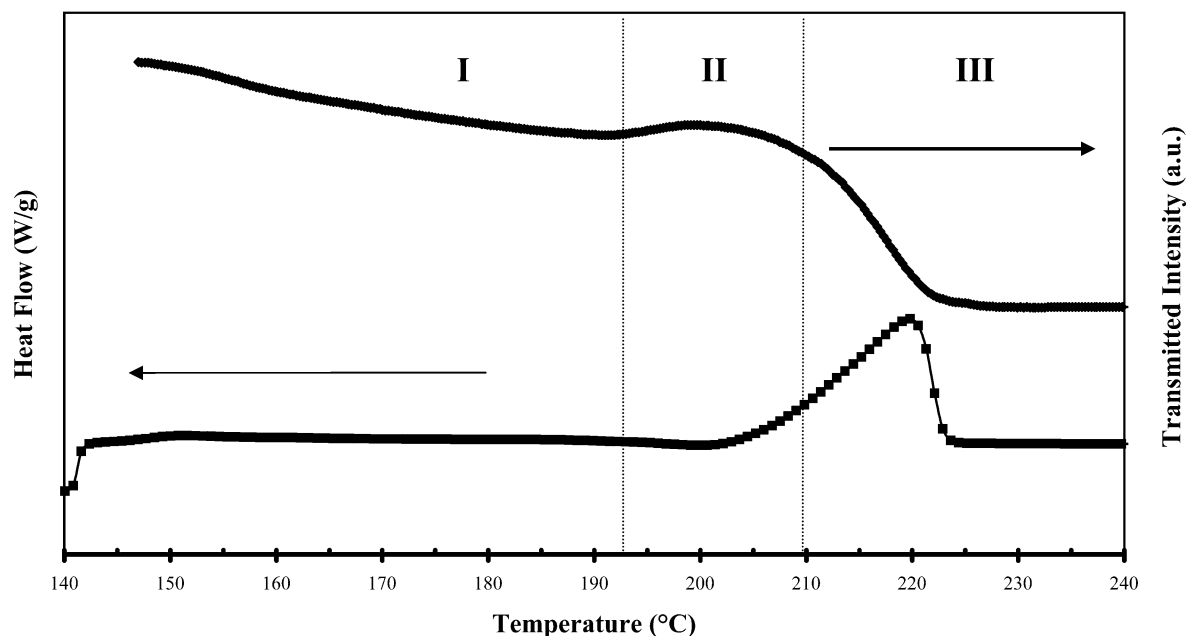


Figure 6. Depolarized light intensity decay and DSC heating traces of low molecular weight nylon-6 after isothermal crystallization (140 °C; 1 h).

during the heating process. The results are shown in Figure 5, which is a DSC scan of a sample crystallized at 120 °C for 60 min, the WAXD patterns in the inset being characteristic of the temperatures during heating. Most obvious is the lack of crystallographic change following the small first melting endotherm. Interestingly, the recrystallization zone does not seem to involve crystal perfection as the WAXD pattern does not look sharper. Therefore, the recrystallization mechanism could be associated, for example, with crystal thickening (see SAXS results later). The second endotherm represents melting of the γ form. However, it is also observed (section D of Figure 5) that part of the crystals recrystallize to the more stable α form. This unexpected

change is a clear indication that the second melting endotherm developed by nylon-6 is a complex sequence of melting and recrystallization to a different crystalline structure. No less important, it is also clear that the last melting endotherm (section D) is associated with melting of the α form.

In general, the isothermal crystals are able to recrystallize to the more stable α form on heating, the amount of recrystallization being proportional to the amount of the less stable γ form. For example, for a small γ crystal content, after isothermal crystallization at low temperatures (160 °C), the thermal trace shows only one high melting endotherm (III; 220 °C) since there was recrystallization to the α form. On the other hand, for a high

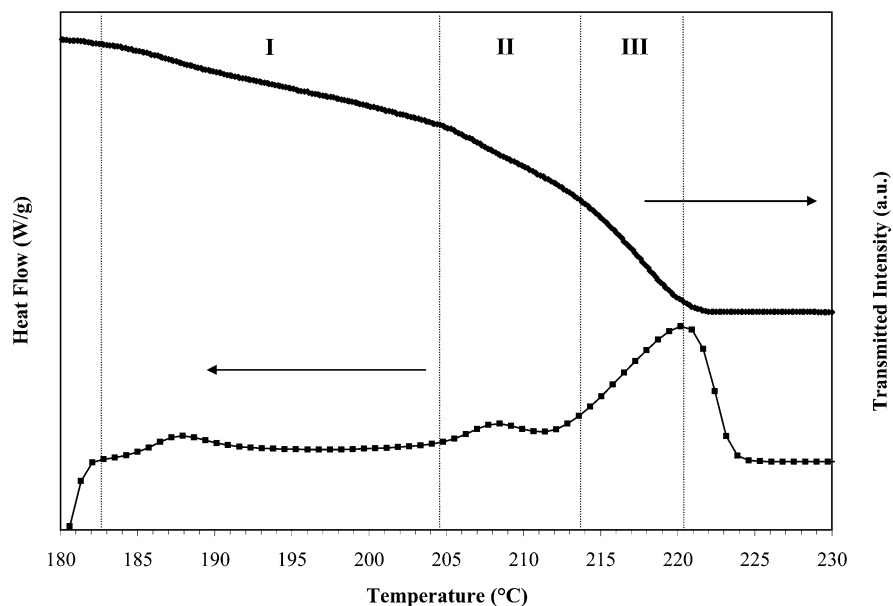


Figure 7. Depolarized light intensity decay and DSC heating traces of low molecular weight nylon-6 after isothermal crystallization (180 °C; 1 h).

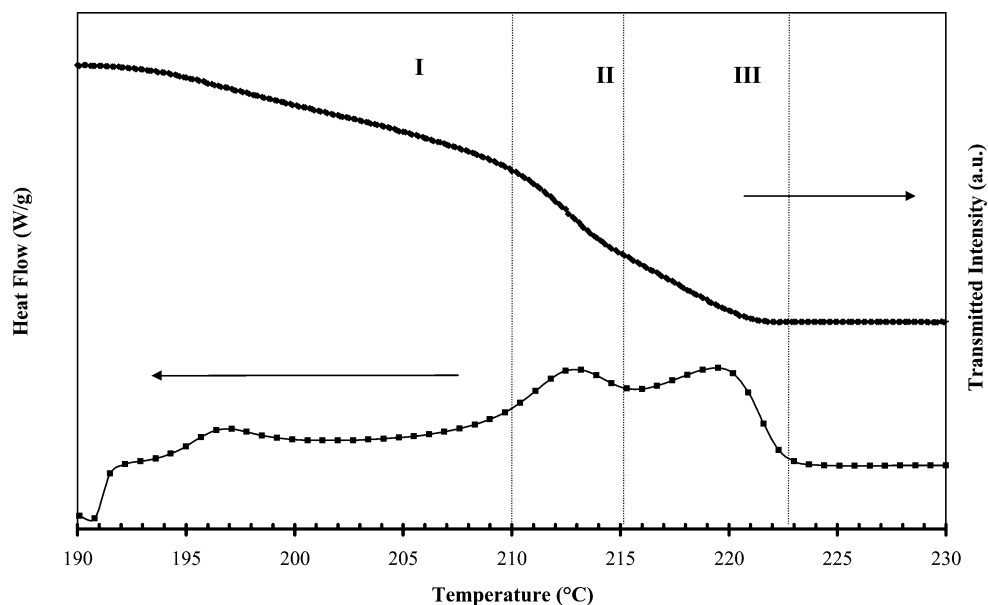


Figure 8. Depolarized light intensity decay and DSC heating traces of low molecular weight nylon-6 after isothermal crystallization (190 °C; 1 h).

content of isothermal γ crystals (100 °C), the thermal trace shows two melting endotherms, one at 212 °C (II) and the other at 220 °C (III), since only part of the γ structure recrystallized to the α habit. The stable α form shows triple melting patterns, which follow the well-known thermal sequence of double, triple, double melting behavior.

Steplike Melting Behavior. The behavior of the most stable α crystalline form generated with the low molecular weight nylon-6 was studied using optical microscopy and a photosensor in order to gain insight into the melting mechanism. Figures 6–8 show the variation of heat flow (DSC) and transmitted light intensity with increasing temperature for selected isothermal crystallization temperatures. To cover as wide a range of crystallization behavior as possible, the selected temperatures were 140 °C (beginning of double melting), 180 °C (beginning of triple melting), and 190 °C (well-defined triple melting). The results for isother-

mal crystallization at 140 °C (Figure 6) indicate a continuous decrease (step I) in light transmitted up to temperatures before the recrystallization exotherm. Since this range covers the first melting endotherm, the result shows that this endotherm must involve melting of a morphological feature. Following this decay step, a high increase in light transmitted, originating from recrystallization, took place (step II). However, following this last increase there was a light intensity decay due to melting of the recrystallized crystals (step III).

Figure 7, on the other hand, corresponds to melting after isothermal crystallization at 180 °C and shows somewhat different behavior. Here there is clearly a three-step-like melting mechanism with sequential decay intensities (I–II–III) during heating. These last results are similar to the ones shown in Figure 8, for isothermal crystallization at 190 °C, which also show the same general type of behavior, although the magnitudes of the peaks differ. In this last case, however, a

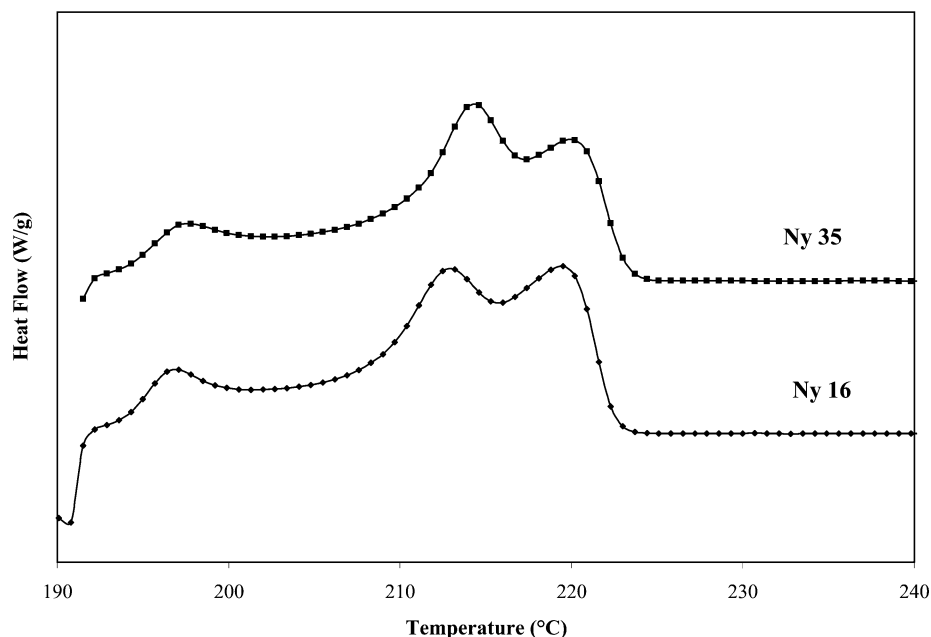


Figure 9. DSC heating traces after isothermal crystallization (190 °C; 1 h) of low molecular weight nylon-6 (Ny16) and high molecular weight nylon-6 (Ny35).

Table 1. Nylon-6 Interface Distribution Function SAXS Results after Isothermal Crystallization at the Temperature of 160 °C and Specifically Selected Heating Temperatures^a

temp (°C)	L (nm)	l_1 (nm)	l_2 (nm)
160	6.7	2.6	4.1
200	6.9	2.8	4.1
211	7.5	3.3	4.2

^a L = long periodicity, l_1 = lamellar thickness, and l_2 = amorphous thickness.

sharper II–III transition is observed coincident with the presence of a higher second melting endotherm. Even though they could be present during scanning,²⁰ recrystallization events were not detected in the last two experiments. In summary, the previous results are a clear indication that the α form follows a sequential steplike melting behavior just as in the case of PET homopolymers¹¹ and P(ET/CT) copolymers.¹²

The Recrystallization Exotherm. To determine the origin of the recrystallization exotherm around 203 °C, observed after heating the isothermal crystals generated at 160 °C from the low molecular weight sample, the one-dimensional interface distribution function¹⁸ was determined using SAXS after heating–quenching the corresponding samples at selected temperatures. Here, we consider the $g_1(r)$ observable peak as associated with the average lamellar thickness, since nylon-6 is a low crystallinity polymer, which is expected to generate large amorphous areas. This was considered so even though crystal sizes are only about three crystallographic repeats. The results are shown in Table 1, and it is clearly observed that the recrystallization exotherm is associated with thicker lamellae, which increase on average 27%. (The corresponding WAXD patterns not shown here always indicated α crystals.) It needs to be mentioned however²³ that in PET (a low crystallinity polymer) the larger value of the two correlation lengths emerging from SAXS calculations is assigned to the lamellar thickness. Therefore, if we consider the larger value of the correlation lengths in order to support our ideas, the effect is still there; however, it is not as clear as with the low correlation length.

Molecular Weight Effects. As indicated before, several hypotheses have been given in the past to explain the origin of multiple melting endotherms in semicrystalline single-crystal habit polymers (for a review see ref 12). One of these hypotheses has however used the approach of comparing the nature of the same or different polymers rather than comparing results emerging from different experimental techniques. This morphological approach has generated the so-called steplike crystallization and melting mechanism which has successfully explained the behavior of the DSC traces of PET homopolymers and random P(ET/CT) exclusion copolymers.^{11,12} A more elaborate explanation for the melting process, on the basis of this mechanism, has also recently been proposed.²²

The effect of molecular weight on the behavior of PET¹¹ was explained as one where large molecules on crystallization generate a higher number of rejected loops from the main crystals than do small molecules. This effect promotes the amount of secondary crystallization through secondary branching and, in terms of the hypothesis, increases the magnitude of the second melting endotherm observed under PET triple melting conditions. Nylon-6, as shown before, is a highly complicated system due to the polymorphism involved in its crystallization. However, if the behavior of nylon-6 is compared in terms of molecular weight, just as with PET, but at constant crystal habit (the most stable α generated at 190 °C; 1 h), then it is possible to observe, as shown in Figure 9, that the indicated hypothesis can also be applied to nylon-6; i.e., the second melting endotherm is clearly enhanced by higher molecular weight.

The morphological studies summarized in Figure 10 corroborate the previous propositions. Figure 10A shows crystallization results (100 °C; pseudo α) of the low molecular weight sample. Here a thin crystal grain is observed with a very low amount of secondary crystallization (infilling effects). Increasing the crystallization temperature to 190 °C (well-developed α), as shown in

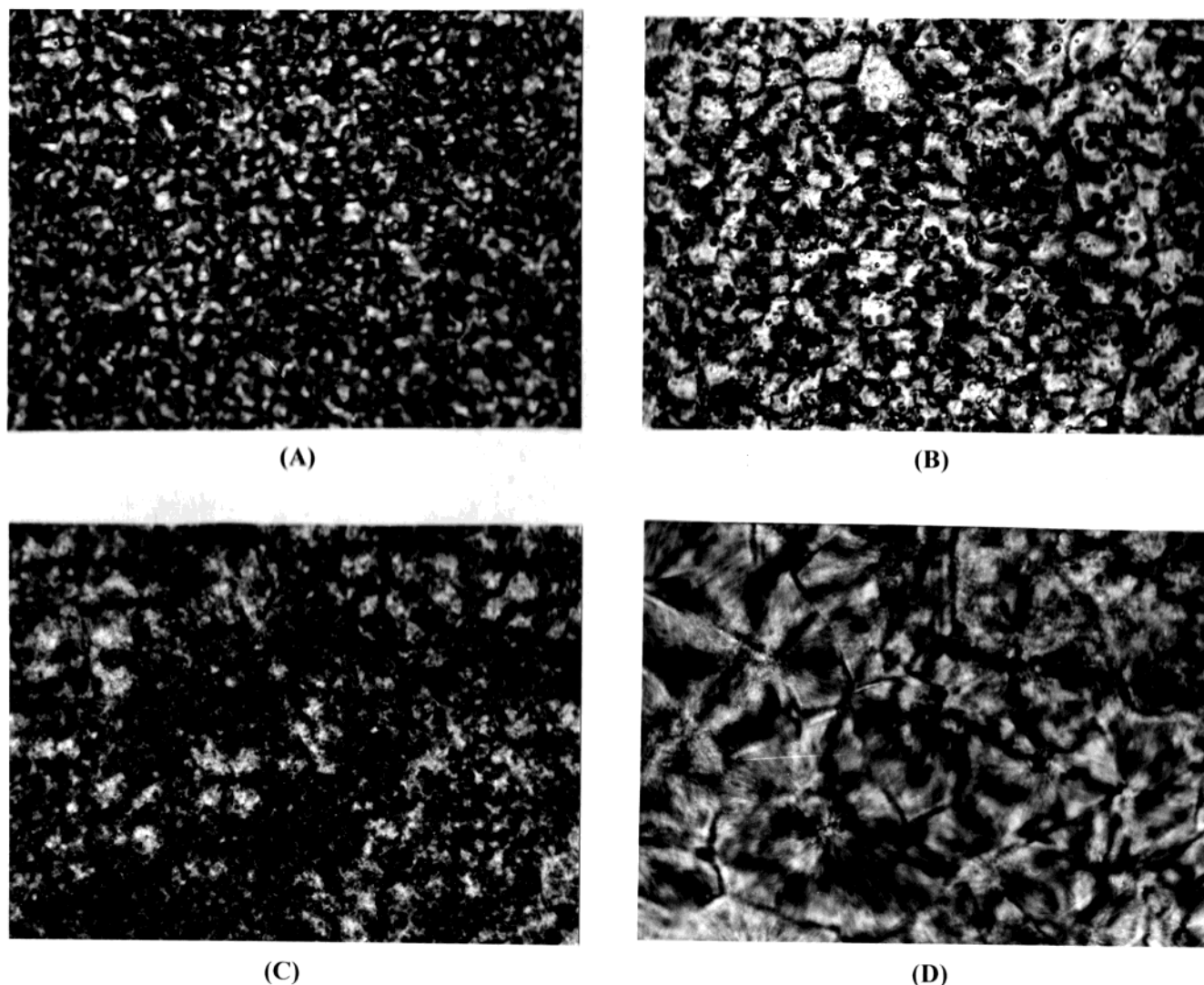


Figure 10. Nylon-6 micrographs (20 \times) after isothermal crystallization from the melt of low molecular weight nylon-6 (A, 100 $^{\circ}$ C; B, 190 $^{\circ}$ C) and high molecular weight nylon-6 (C, 100 $^{\circ}$ C; B, 190 $^{\circ}$ C) showing differences in morphology and secondary crystallization.

Figure 10B, leads to better-defined crystals with larger size but still lower amounts of secondary crystallization. Increasing the molecular weight and crystallizing at 100 $^{\circ}$ C (Figure 10 C, well-developed γ) leads to a combination of large crystals with low amount of secondary crystallization and large crystalline areas with unresolved morphology. However, an increase in crystallization temperature to 190 $^{\circ}$ C (well-developed α) (Figure 10D) leads to well-defined large crystals with a high amount of secondary crystallization.

As for the isothermal crystals, SAXS experiments of the different molecular weight samples were carried out after isothermal crystallization at different temperatures. Room temperature SAXS patterns did show a difference in the invariant Q (total scattering intensity) when the different molecular weight samples were compared, as shown in Figure 11. At low crystallization temperatures (i.e., up to 140 $^{\circ}$ C), there were two different crystalline structures, and the low molecular weight sample (mostly α) did show a lower invariant. However, above the isothermal crystallization temperature of 180 $^{\circ}$ C, the high molecular weight sample had a faster increase in the total scattering intensity as an indication of a higher content of secondary crystals.^{11,12} As shown before, above 180 $^{\circ}$ C there is only the α crystal

habit in both samples (i.e., where the triple DSC melting sequence begins to manifest itself). Therefore, within the context of the steplike melting mechanism, the second melting endotherm of the DSC traces in α nylon-6 must be associated with secondary crystalline structures emerging from the primary crystals which give rise to a higher invariant, as has been reported before.¹¹

It is recognized that there is a change in crystal structure occurring in the temperature range of study, normally referred to as the Brill transition,^{24,25} which in nylon-6 is now believed to be a change in the monoclinic crystal structure, rather than a change in the basic unit cell. The Brill transition has been proposed to exist for nylon-6,6 and nylon-6. However, in both cases, it has been shown that the nature of the transition is different in a number of ways.²⁴ In the particular case of nylon-6, the α form generates a new α' form with two diffraction peaks at around 160 $^{\circ}$ C, i.e., the Brill transition. This transition is different in nature and opposite in behavior if some similarity is pretended to be found with the present study. In our study, and as a function of crystallization temperature, or linear heating, we observed a crystal-to-crystal change from the γ form to the more stable α form. A

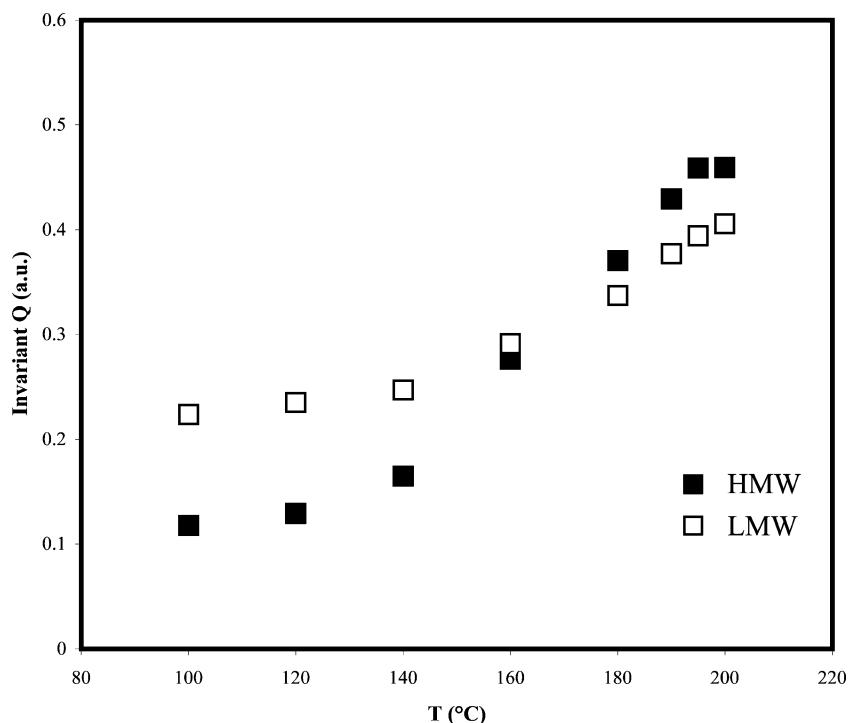


Figure 11. Invariant as a function of isothermal crystallization (1 h) of low molecular weight nylon-6 (LMW) and high molecular weight nylon-6 (HMW).

transition between these two forms can be observed at 160 °C (a casual coincidence with the Brill transition) with the high molecular weight sample. Librational motion of nitrogen and carbon groups in crystalline domains below and above Brill transitions has been determined for nylon-6,6.²⁶ There has not been a report of librational motion for nylon-6, therefore, considering that the Brill transition is rather different in both polymers and also considering that the results here presented do not have any direct connection with the Brill transitions, librational motions, or their influence to explain our results, should be discarded. In other words, the study reported here shows no discernible changes that can be associated with the Brill transition, and hence, it appears that such transition in this polymer has little or no influence on the morphological events being reported.

Conclusions

The complex melting behavior of nylon-6 is strongly dependent on molecular weight. However, other than the well-known molecular weight effects on crystallization of polymers, the main observed effect in the present study was the formation of different crystal habits as a function of molecular weight.

The melting behavior of nylons is not a particular behavior of this family of polymers since under specific conditions it can follow typical patterns shown by other semicrystalline systems, such as PET homopolymers, P(ET/CT) copolymers, and potentially other high-temperature polymers.

Out of the transition zone (where up to four melting endotherms can be observed), nylon-6 is able to develop up to three melting endotherms which can be explained as follows. The first melting endotherm is a morphological manifestation of the last steps of secondary crystallization; the second melting endotherm is mainly associated with melting of the γ form, although there is a parallel recrystallization process to the α form. The third

melting endotherm is associated with melting of the α crystalline form.

Nylon-6 is able to recrystallize on heating from the less stable γ form to the most stable α form; however, there is not a correlation between this type of recrystallization and that where a small recrystallization exotherm is commonly observed, the latter being associated with an increase in lamellar thickness.

Acknowledgment. The financial support of this work was provided by a grant from CONACYT, Mexico (495100-5-C087A), and FAI/UASLP/México. The research at Oak Ridge was sponsored in part by the U.S. Department of Energy under Contract DE-AC05-00OR22725 with the Oak Ridge National Laboratory, managed by the UT-Battelle, LLC. The contribution from the University of Tennessee is supported by the Polymers program of NSF under Grant DMR 0096505.

References and Notes

- (1) Brill, R. Z. *Phys. Chem. B* **1943**, 53, 61.
- (2) Holmes, R.; Bunn, D. W.; Smith, D. J. *J. Polym. Sci.* **1955**, 17, 159–177.
- (3) Arimoto, H.; Ishibashi, M.; Hirai, M.; Chatani, Y. *J. Polym. Sci., Part A* **1965**, 3, 317–326.
- (4) Liberty, F. N.; Wunderlich, B. *J. Polym. Sci., Part A-2* **1968**, 6, 833–848.
- (5) Illers, V. K. H.; Haberkorn, H. *Makromol. Chem.* **1971**, 142, 31–67.
- (6) Arakawa, T.; Nagatoshi, F.; Arai, N. *J. Polym. Sci., Part A-2* **1969**, 1461–1472.
- (7) Privalko, V. P.; Kawai, T.; Lipatov, Yu. S. *Polym. J.* **1979**, 11, 669–709.
- (8) Martuscelli, E.; Riva, F.; Sellitti, C.; Silvestre, C. *Polymer* **1985**, 26, 270–282.
- (9) Khana, Y. *Macromolecules* **1992**, 25, 3298–3300.
- (10) Medellín-Rodríguez, F. J.; Phillips, P. J.; Lin, J. S. *Macromolecules* **1996**, 29, 7491–7501.
- (11) Medellín-Rodríguez, F. J.; Phillips, P. J.; Lin, J. S.; Campos, R. J. *Polym. Sci., Part B: Polym. Phys.* **1997**, 35, 1757–1774.

- (12) Medellín-Rodríguez, F. J.; Phillips, P. J.; Lin, J. S.; Avila-Orta, C. A. *J. Polym. Sci., Part B: Polym. Phys.* **1998**, *36*, 763–781.
- (13) Wunderlich, B. In *Thermal Analysis*; Academic Press: New York, 1990; p 424.
- (14) Wignall, G. D.; Lin, J. S.; Spooner, S. *J. Appl. Crystallogr.* **1990**, *23*, 241–252.
- (15) Hendricks, R. W. *J. Appl. Crystallogr.* **1978**, *11*, 15–23.
- (16) Debye, P.; Anderson, H. R., Jr.; Brumberger, H. *J. Appl. Phys.* **1957**, *28*, 679–683.
- (17) Porod, G. *Kolloid-Z.* **1952**, *125*, 51–57.
- (18) Ruland, W. *Colloid Polym. Sci.* **1977**, *255*, 417–427.
- (19) Gurato, G.; Fichera, A.; Grandi, F. Z.; Zannetti, R.; Canal, P. *Makromol. Chem.* **1974**, *175*, 953–975.
- (20) Miyasaka, K.; Ishikawa, K. *J. Polym. Sci., Part A2* **1968**, *6*, 1317–1329.
- (21) Murthy, N. S. *Polym. Commun.* **1991**, *32*, 301–305.
- (22) Avila-Orta, C. A.; Medellín-Rodríguez, F. J.; Wang, Z.-G.; Navarro-Rodríguez, D.; Hsiao, B. S.; Yeh, F. *Polymer* **2003**, *44*, 1527–1535.
- (23) Xia, Z.; Sue, H. J.; Wang, Z.; Avila-Orta, C. A.; Hsiao, B. S. *J. Macromol. Phys.* **2001**, *B40*, 625–638.
- (24) Murthy, N. S.; Curran, S. A.; Aharoni, S. M.; Minor, H. *Macromolecules* **1991**, *24*, 3215–3220.
- (25) Vasanathan, N.; Murthy, N. S.; Bray, R. G. *Macromolecules* **1998**, *31*, 8433–8435.
- (26) Hirschinger, J.; Miura, H.; Gardner, K. H.; English, A. D. *Macromolecules* **1990**, *23*, 2153–2169.

MA030466C